Journal of
Applied Crystallography
ISSN 0021-8898
Editor: **Anke R. Pyzalla**

Accessible reciprocal-space region for non-coplanar Bragg and Laue geometries

Oleksandr Yefanov

J. Appl. Cryst. (2008). **41**, 110–114

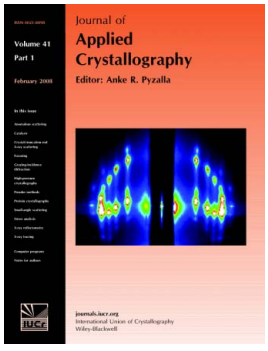

Journal of
Applied Crystallography
ISSN 0021-8898

Received 26 June 2007
Accepted 4 October 2007

Accessible reciprocal-space region for non-coplanar Bragg and Laue geometries

Oleksandr Yefanov

V. Lashkarev Institute of Semiconductor Physics, 45 Nauky Ave., Kiev 03680, Ukraine.
Correspondence e-mail: efa@hotbox.ru

Accurate shapes of the accessible reciprocal-space region for non-coplanar Bragg and Laue geometries are given. Vector formulae for finding these regions and for experimental geometry calculations for obtaining diffraction from any accessible (using a given wavelength) reciprocal node are presented. A method for converting these formulae to scalar equations is proposed. Solutions are given and illustrated as three-dimensional figures in reciprocal space.

1. Introduction

Modern semiconductor electronics use increasingly complicated structures, such as multilayers with quantum wires and quantum dots. An investigation of the geometrical and structural parameters of such structures by X-rays requires a non-coplanar experimental geometry (Schmidbauer, 2004; Pietsch *et al.*, 2004) where the incident beam, the diffracted beam and the surface normal are not in the same plane. For this reason, the task of finding a suitable geometry for the diffraction experiment is vital. Of course, only reciprocal nodes that can be accessed under the current experimental conditions should be considered. Therefore, the correct shape of the accessible reciprocal-space region needs to be determined.

This shape in the case of coplanar Bragg geometry (Fig. 1) is well known (Bowen & Tanner, 1998). But for the non-coplanar case, it is often plotted incorrectly (Fig. 2) [see, for example, Schmidbauer (2004) or Stangl *et al.* (2004)]. Here, the correct three-dimensional accessible region is constructed for both the Bragg and the Laue geometry on the basis of appropriate vector equations. The proposed equations can also be used for finding a suitable experimental geometry for measuring diffraction from a given reciprocal node.

2. Basic principles

Basic geometrical considerations are as follows. $\mathbf{K}_0$ is the beam incident on the crystal (red in the figures) and $\mathbf{K}_h$ is the diffracted beam (green); the crystal surface is defined by its outer normal vector $\mathbf{N}$, and the plane of incidence (the plane where $\mathbf{N}$ and $\mathbf{K}_0$ lie) is given by its normal vector $\mathbf{P}$ [see equation (4)]. The end of vector $\mathbf{K}_0$ points to the origin of the coordinate system. The diffracted beam is connected to the incident beam by equation (3), where $\mathbf{Q}$ is a reciprocal-space vector drawn from the origin of the coordinate system to the reciprocal point under investigation. In the case of elastic scattering and at a given wavelength λ, the conditions of equations (1) and (2) must be fulfilled, where $K = 1/\lambda$. The incident beam $\mathbf{K}_0$ must fall on the crystal surface from a vacuum [its projection on $\mathbf{N}$ is negative; equation (5)]. If the diffracted beam $\mathbf{K}_h$ exits from the same side of the crystal as $\mathbf{K}_0$ enters [the projection of $\mathbf{K}_h$ on $\mathbf{N}$ is positive; equation (6)], this is called Bragg geometry; in the opposite case, this is referred to as Laue geometry [equation (7)].

For a given direction of $\mathbf{K}_0$, the possible ends of vector $\mathbf{K}_h$ (and vector $\mathbf{Q}$) lie on the Ewald sphere with radius K (Fig. 3), so if $\mathbf{K}_0$ takes all possible positions in the plane of incidence

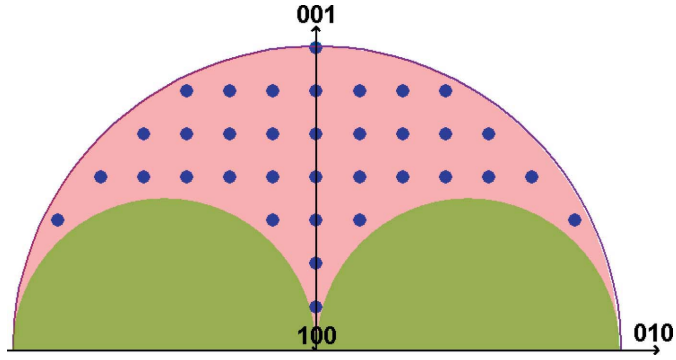

Figure 1
Accessible region in reciprocal space for the coplanar Bragg case.

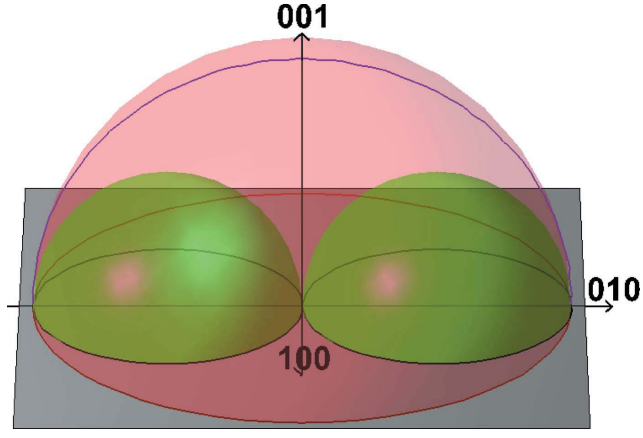

Figure 2
Incorrect accessible region for the non-coplanar Bragg geometry as plotted in some books.

and equation (5) is fulfilled, the possible ends of vector $\mathbf{K}_h$ and $\mathbf{Q}$ lie inside the volume shown in Fig. 4 (for positive Q_z this is half of a torus, while for negative Q_z it is two hemispheres with radius K), and not in a sphere with radius $2K$, as is usually considered (red in Fig. 2). This means that for a given plane of incidence and wavelength, all reciprocal nodes that lie outside the volume in Fig. 4 cannot be accessed. Certainly, if the plane of incidence is not considered, the accessible region for Bragg geometry is a hemisphere with radius $2K$, but in this case no small hemispheres could be drawn (green in Fig. 2), because the centres of these small hemispheres always belong to the plane of incidence. For Laue geometry there is no such hemisphere with radius $2K$, as will be shown later in this article.

3. Main equations

The main equations for building the accessible reciprocal-space region are:

$$|\mathbf{K}_0| = K, \tag{1}$$

$$|\mathbf{K}_h| = K, \tag{2}$$

$$\mathbf{K}_h = \mathbf{K}_0 + \mathbf{Q}, \tag{3}$$

$$(\mathbf{K}_0 \cdot \mathbf{P}) = 0, \tag{4}$$

$$(\mathbf{K}_0 \cdot \mathbf{N}) \leq 0. \tag{5}$$

For Bragg geometry:

$$(\mathbf{K}_h \cdot \mathbf{N}) > 0. \tag{6}$$

For Laue geometry:

$$(\mathbf{K}_h \cdot \mathbf{N}) < 0. \tag{7}$$

In the case when $(\mathbf{K}_h \cdot \mathbf{N}) = 0$, both Bragg and Laue geometries must give the same result.

The problem of solving these equations is simplified greatly if all vectors are expressed in a Cartesian coordinate system, where axis z is parallel to the crystal surface normal and axis x belongs to the plane of incidence. Then vectors $\mathbf{N}$, $\mathbf{P}$ and $\mathbf{K}_0$ are: $\mathbf{N} = (0, 0, N_z)$; $\mathbf{P} = (0, P_y, 0)$; $\mathbf{K}_0 = (K_{0x}, 0, K_{0z})$. The translation from any Cartesian coordinate system to that described here can be made with the help of up to two rotations (Casanova, 1976). For greater simplicity, vectors $\mathbf{N}$ and $\mathbf{P}$ could be set as unit vectors: $|\mathbf{N}| = N_z = 1$ and $|\mathbf{P}| = P_y = 1$.

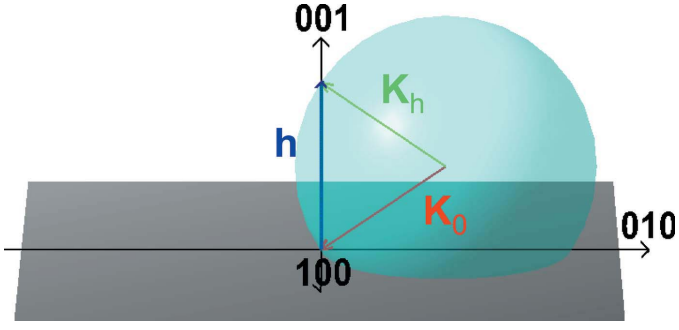

Figure 3
For fixed $\mathbf{K}_0$ (red), all possible ends of vector $\mathbf{K}_h$ (green) form a sphere.

4. Results and discussion

When considering equations (1)–(7) in scalar form, some quadratic or biquadratic equations for the unknown variable Q_z, for example, can be found (see Appendix *A*). In Figs. 5 and 6, the final view of the allowed reciprocal-space region for the Bragg and the Laue case, respectively, are shown. Considering the structure factor F_h for each reciprocal node, one quarter of the figure for the Bragg case and a silicon crystal is shown in Fig. 7 (the diameter of each point is proportional to F_h). This could be useful for taking into account only those reciprocal

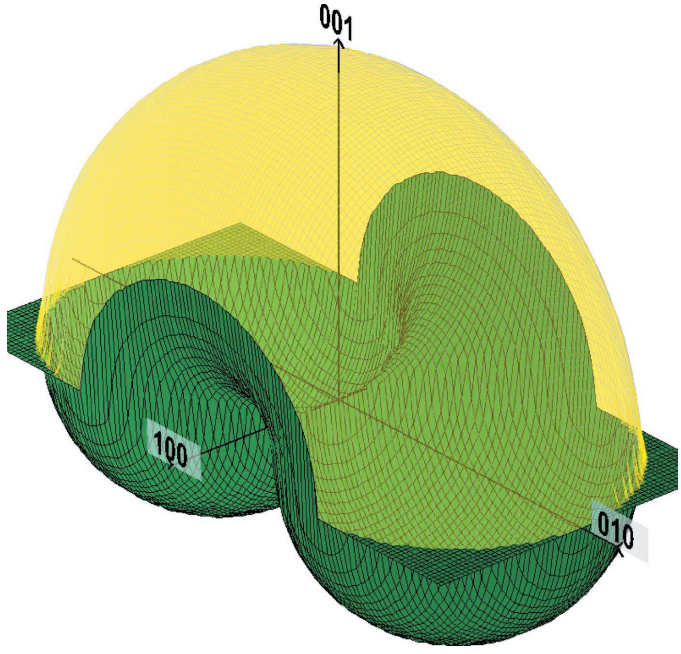

Figure 4
All fundamentally accessible reciprocal points, for a fixed plane of incidence, lie inside this volume.

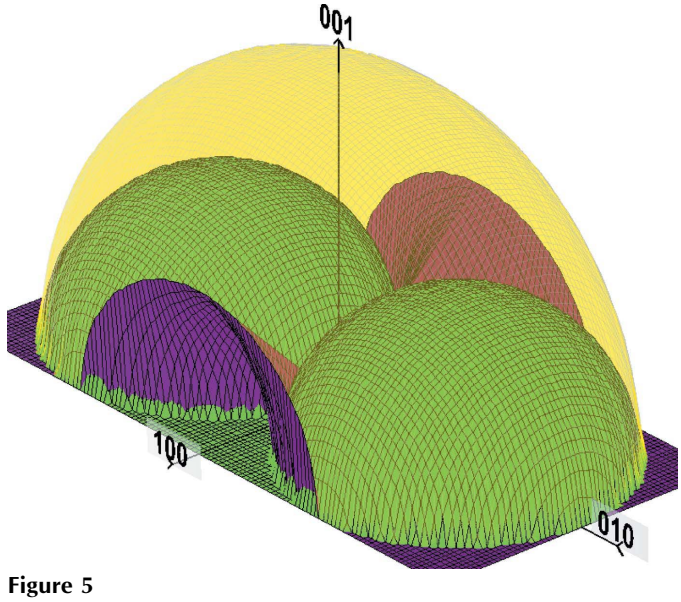

Figure 5
The correct accessible reciprocal-space region for Bragg geometry with a fixed incidence plane.

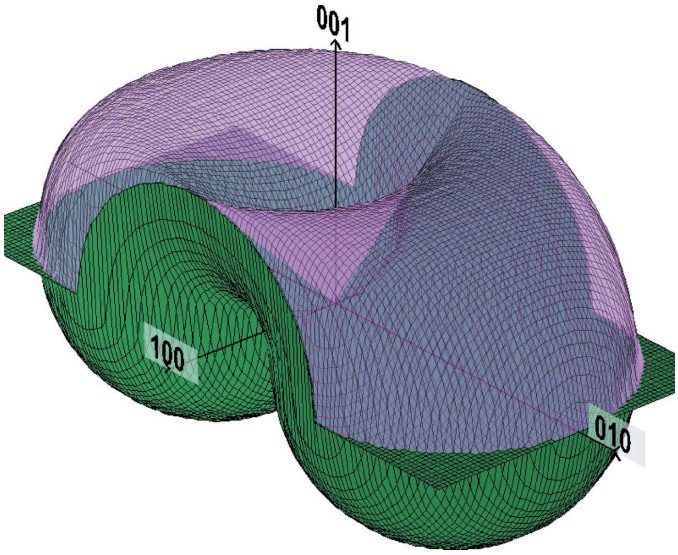

Figure 6
The correct accessible reciprocal-space region for Laue geometry with a fixed incidence plane.

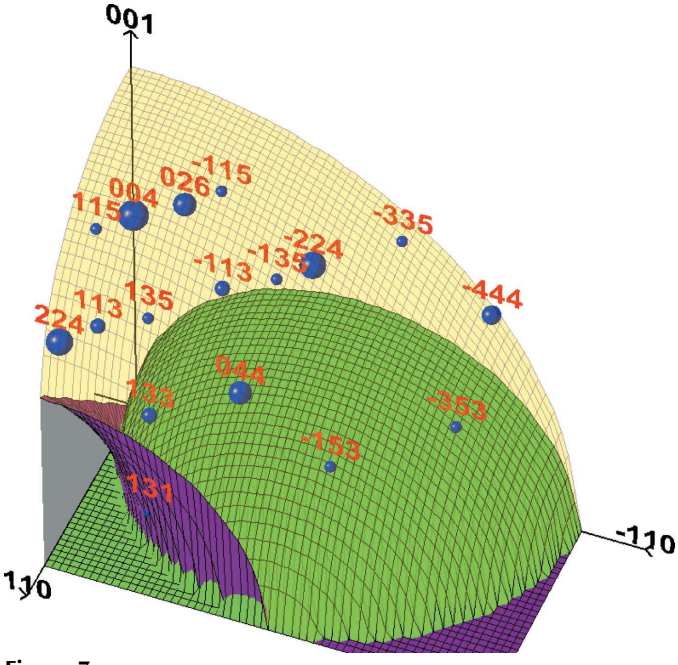

Figure 7
A quarter of the accessible region for Bragg geometry with an Si [001] crystal and λ = 1.54 Å. The size of each point (blue) is proportional to the Si structure factor.

nodes that give valuable diffracted intensity. The structure factor was calculated using the open-source library *HiCalc* (Saveleva *et al.*, 2006).

The correct shape of the reciprocal-space region in Bragg geometry can be explained rather easily. For any $\mathbf{K}_0$ (of course $K_{0z} \leq 0$) allowed in the Bragg case, the possible ends of vector $\mathbf{K}_h$ form an empty hemisphere (because $K_{hz} \geq 0$) of radius K with the centre at the beginning of vector $\mathbf{K}_0$ (two such hemispheres for $K_{0z} = 0$ are shown in Fig. 5 in green). Then this hemisphere is plotted for all possible positions of $\mathbf{K}_0$ in the plane of incidence; the figure between the yellow and green/purple surfaces in Fig. 5 is obtained. The yellow surface is, of course, the upper part of a torus, and the purple surface is determined by the condition $K_{hz} = 0$.

The equations described above can be used for other useful purposes. For example, to find the incident and diffracted beams for any reciprocal point, equation (2) could be modified using equation (3):

$$(\mathbf{K}_0 \cdot \mathbf{Q}) = -Q^2/2. \tag{8}$$

Then, using equations (1), (4) and (8), vector $\mathbf{K}_0$ can be found easily, and thus by using equation (3), vector $\mathbf{K}_h$ is determined (for the final formulae see Appendix *A*). Another use of the proposed equations is in the determination of the direction in which vector $\mathbf{K}_0$ should be set to achieve diffraction from a reciprocal point with vector $\mathbf{Q}$. For this purpose, vector $\mathbf{Q}$ should be set, and vector $\mathbf{P}$ could be found from equations (1)–(7).

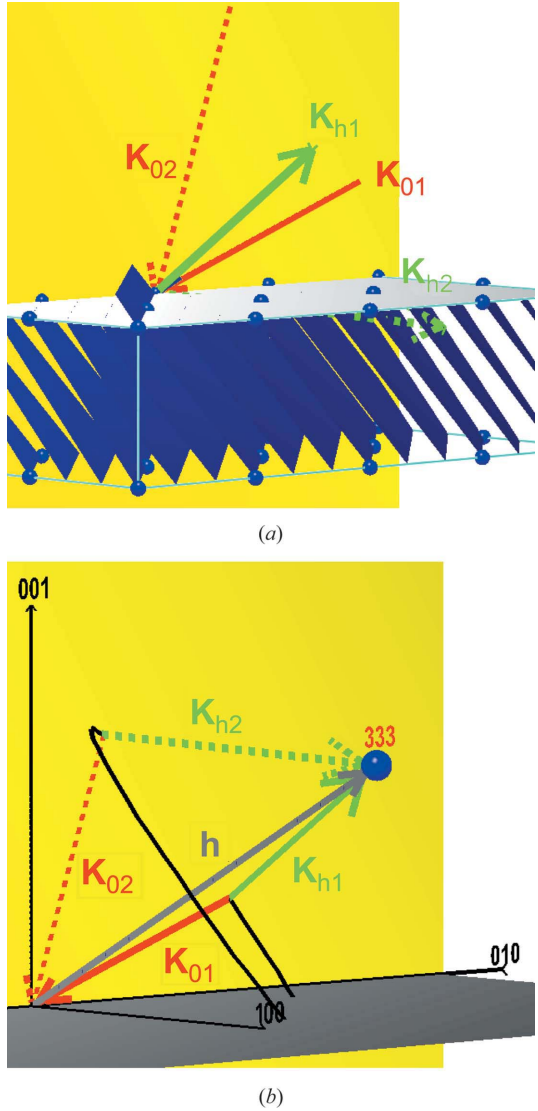

Figure 8
Two possible beam paths to reach the 333 reciprocal node (blue point) for an Si [001] crystal and incident beam (red) in the (100) plane (yellow). Diffracted beams: green. (*a*) Real space. (*b*) Reciprocal space.

For any given reciprocal point with vector **Q**, diffraction occurs when the origins of vectors $\mathbf{K}_0$ and $\mathbf{K}_h$ lie on a circle that is formed by rotation of these vectors around vector **Q** (black curve in Fig. 8*b*). Thus, in most cases, for a given reciprocal point and plane of incidence, there are two possible beam paths (solid and dashed lines in Fig. 8). Therefore, some of the reciprocal points could be reached in both the Bragg and the Laue geometry (Fig. 8*a*) and these points belong to both the Bragg and the Laue accessible regions (Figs. 5 and 6).

As was pointed out at the beginning of this article, all the regions described are plotted for a fixed plane of incidence, which means that the azimuthal angle of the incident beam is fixed. If this angle changes, all reciprocal points inside the hemisphere with radius $2K$ (red in Fig. 2) could be accessed in the Bragg geometry. In this case, all fundamentally accessible points for the Laue geometry lie inside a horizontal torus. If the angle of incidence (between the beam and the surface) is constant, which is usually the case for grazing-incidence experiments, the fundamentally accessible region in the Bragg geometry for an arbitrary plane of incidence is the volume plotted in Fig. 9.

All figures in this article were plotted with the program *XViz* (Yefanov, 2007) using the *TeeChart7* component (Steema, 2006). For a better understanding of the shapes of these figures, the reader is referred to http://x-ray.net.ua/xviz.html, where animated pictures can be found. The correctness of Figs. 4–7 can be easily checked with the program *XViz* by plotting beam paths for any reciprocal node, as shown in Fig. 8.

APPENDIX *A*
Main formulae in Cartesian coordinates

For a given reciprocal point with vector **Q** ($|\mathbf{Q}| = Q \leq 2K$) and a plane of incidence with normal **P**, the incident beam vector $\mathbf{K}_0$ can be found by solving the following equations:

$$\begin{aligned}&[(Q_yP_z - P_yQ_z)^2 + (Q_zP_x - P_zQ_x)^2 + (Q_yP_x - P_yQ_x)^2]K_{0x}^2\\ &\quad - Q^2[Q_zP_xP_z + Q_yP_xP_y - Q_x(P_y^2 + P_z^2)]K_{0x}\\ &\quad + Q^4(P_y^2 + P_z^2)/4 - K^4(Q_yP_z - P_yQ_z)^2 = 0,\end{aligned} \tag{9}$$

$$K_{0y} = \frac{-P_zQ^2/2 + (P_xQ_z - P_zH_x)K_{0x}}{P_zH_y - P_yH_z}, \tag{10}$$

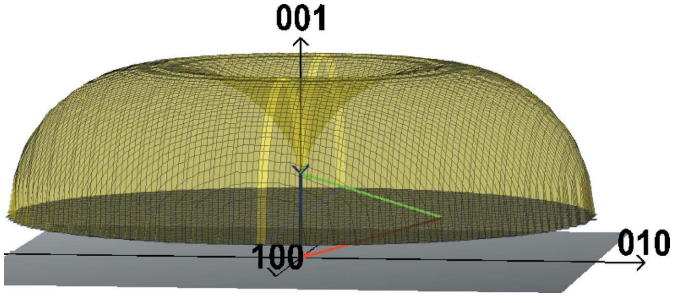

Figure 9
For a fixed incidence angle, all accessible reciprocal points lie inside this volume.

$$K_{0z} = \frac{-P_yQ^2/2 + (P_xQ_y - P_yH_x)K_{0x}}{P_yH_z - P_zH_y}. \tag{11}$$

The diffracted beam $\mathbf{K}_h$ is then:

$$K_{hx} = K_{0x} + Q_x, \quad K_{hy} = K_{0y} + Q_y, \quad K_{hz} = K_{0z} + Q_z. \tag{12}$$

When considering a simplified coordinate system, where vectors $\mathbf{N} = (0, 0, 1)$, $\mathbf{P} = (0, 1, 0)$, $\mathbf{K}_0 = (K_{0x}, 0, K_{0z})$, equations (9)–(11) take the form:

$$(Q_z^2 + Q_x^2)K_{0x}^2 + Q^2Q_x^2K_{0x} + Q^4/4 + K^4Q_z^2 = 0, \tag{13}$$

$$K_{0y} = 0, \qquad K_{0z} = \pm(K^2 - K_{0x}^2)^{1/2}. \tag{14}$$

In the coordinate system described, the equation for the fundamentally accessible reciprocal points (half of a torus for $Q_z > 0$ in Fig. 4, yellow surface in Fig. 5 and green surface for $Q_z > 0$ in Fig. 6) takes the form (here and later $-2K \leq Q_x \leq 2K$ and $-K \leq Q_y \leq K$ are set and Q_z is calculated):

$$Q_z^4 + 2(Q_x^2 + Q_y^2 - 2K^2)Q_z^2 + (Q_x^2 + Q_y^2)^2 - 4K^2Q_x^2 = 0. \tag{15}$$

Only positive Q_z should be considered, because the surface for $Q_z < 0$ is determined by equation $K_{0z} = 0$, as described below.

The equation for the surface where $\mathbf{K}_h$ is parallel to the crystal surface ($K_{hz} = 0$) is

$$Q_z^4 + 2(Q_x^2 - Q_y^2)Q_z^2 + (Q_x^2 + Q_y^2)^2 - 4K^2Q_x^2 = 0\,. \tag{16}$$

One solution of this equation is plotted in light purple in Fig. 6 and the other in purple in Fig. 5. Two other roots are negative and non-accessible due to the presence of the surface, described below.

The equation for the surface where $\mathbf{K}_0$ is parallel to the crystal surface ($K_{0z} = 0$) is

$$Q_z^2 = -Q_x^2 - Q_y^2 + 2K|Q_x|\,. \tag{17}$$

The roots are shown in green in Fig. 5 ($Q_z > 0$) and in Fig. 6 ($Q_z < 0$).

For a fixed angle of incidence (K_{0z} = constant), the surface is described by ($-2K \leq Q_y \leq 2K$)

$$Q_z^2 + 2K_{0z}Q_z + Q_x^2 + Q_y^2 - 2[(K^2 - K_{0z}^2)(Q_x^2 + Q_y^2)]^{1/2} = 0. \tag{18}$$

The solution for $Q_z \geq K_{0z}$ (Bragg case) is shown in Fig. 9 in yellow.

The author acknowledges his scientific supervisor Kladko Vasyl Petrovich.

References

Bowen, D. K. & Tanner, B. K. (1998). *High Resolution X-ray Diffractometry and Topography*. New York: Taylor and Francis.
Casanova, G. (1976). *L'Algèbre Vectorielle*. Paris: Presses Universitaires de France.
Pietsch, U., Holy, V. & Baumbach, T. (2004). *High-Resolution X-ray Scattering from Thin Films to Lateral Nanostructures*. New York: Springer.

Saveleva, I., Yefanov, O. M. & Kladko, V. P. (2006). *Open source C++ library for polarizability calculation*, http://x-ray.net.ua/downloads/software/hi.rar.
Schmidbauer, M. (2004). *X-ray Diffuse Scattering from Self-Organized Mesoscopic Semiconductor Structures*. New York: Springer.
Stangl, J., Holy, V. & Bauer, G. (2004). *Rev. Mod. Phys.* **76**, 725–783.
Steema (2006). *SteemaSoftware, TeeChart 7.07 component*, http://www.steema.com/. Steema, Girona, Spain.
Yefanov, O. M. (2007). *Demonstration of reciprocal space constructing, diffraction principles and the dawn of reciprocal space mapping*, http://x-ray.net.ua/downloads/software/xviz.rar.